J Physiol 604.7 (2026) pp 3077–3093

The Journal of Physiology

Pharmacological manipulation of the immediate effects of spinal trauma in neonatal rats reveals a crucial role for TRPV4 receptors

Atiyeh Mohammadshirazi[1,2], Caterina Ciani[1], Francesca Emma Mongelli[1], Rashid Giniatullin[3], Carmen Falcone[1,4] and Giuliano Taccola[1,2]

[1]*Neuroscience Department, International School for Advanced Studies (SISSA), Trieste, Italy*
[2]*Applied Neurophysiology and Neuropharmacology Lab, Istituto di Medicina Fisica e Riabilitazione (IMFR), Udine, UD, Italy*
[3]*A.I. Virtanen Institute, University of Eastern Finland, Kuopio, Finland*
[4]*Department of Biological Sciences, Towson University, Towson, USA*

Handling Editors: Katalin Toth & Justin Dean

The peer review history is available in the Supporting Information section of this article (https://doi.org/10.1113/JP289194#support-information-section).

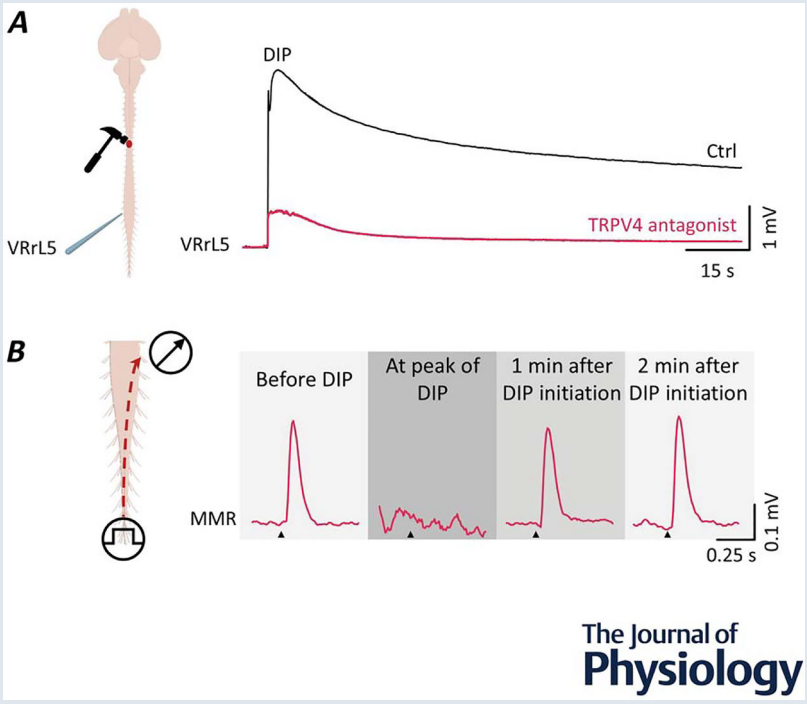

Abstract figure legend *A*, schematic illustration of the ventral aspect of an *ex vivo* preparation of the entire CNS from a neonatal rat subjected to a calibrated thoracic impact. The trauma induced a large depolarising injury potential (DIP, black trace) recorded from the L5 ventral root (VRrL5), which was markedly reduced by transient receptor potential, vanilloid 4 (TRPV4) antagonism (pink trace). ***B***, motor reflex responses (MMRs) recorded from VRrL5 were abolished at the peak of the DIP as a result of spinal shock but recovered within minutes after trauma. TRPV4 antagonism accelerated this recovery, supporting a protective role for TRPV4 blockade in the immediate aftermath of spinal cord injury.

This article was first published as a preprint. Mohammadshirazi A, Taccola G. 2024. An electrophysiological study about the pharmacological manipulation of the immediate consequences of a spinal trauma reveals a crucial role for TRPV4 antagonism. bioRxiv. https://doi.org/10.1101/2024.10.03.616499

DOI: 10.1113/JP289194

Abstract Physical trauma to the spinal cord causes a massive depolarising injury potential (DIP), transient spinal hypoxia and extensive cell loss at the injury site, disrupting conduction along white matter tracts. This leads to transient hypotonia and areflexia during the spinal shock phase. The link between DIP magnitude and spinal cord injury progression, as well as potential pharmacological interventions, remains unexplored, especially in neonatal age. To limit DIP peak and accelerate motor reflex response (MRR) recovery, we applied selective neurochemicals targeting mechanosensitive and classical neurotransmitter receptors. These agents were applied during experimental trauma to the mid-thoracic cord of CNS preparations from 0- to 2.5-day-old rats. Continuous lumbar root recordings monitored baseline levels and MRR elicited by electric pulses to sacro-caudal afferents. In uninjured preparations, each agent affected baseline polarisation, synaptic responses and bursting activity, indicating their role in maintaining the functional state of the spinal cord. Neurochemicals targeting glutamatergic, adenosinergic, glycinergic or GABAergic receptors did not impact trauma outcomes (DIP or MRR). Only the transient receptor potential, vanilloid 4 (TRPV4) antagonist RN1734, not TRPA1 antagonist AP18, reduced DIP peak and accelerated MRR recovery following trauma. The protective effect of RN1734 was corroborated by TRPV4 expression in neonatal spinal neurons and glial cells, located in dura and around the central canal. Blocking gap junctions and $GABA_A$ receptors also restored MRR, but less effectively and more slowly than TRPV4 antagonism. Our findings show that blocking mechanosensitive TRPV4 receptors at the moment of impact effectively reduces the immediate pathological effects of a neonatal spinal trauma.

(Received 30 April 2025; accepted after revision 18 February 2026; first published online 13 March 2026)
Corresponding author G. Taccola: Neuroscience Department, International School for Advanced Studies (SISSA), via Bonomea, 265 - 34136 Trieste, Italy. Email: taccola@sissa.it

Introduction

The initial pathological indicator of a spinal cord injury (SCI) is spinal shock, which manifests as a loss of muscle tone and motor reflexes below the injury site (Ditunno et al., 2004). We have recently described the immediate functional changes occurring as early as 150–200 ms from the onset of a physical trauma to the spinal cord of the entire CNS isolated from neonatal rats (Mohammadshirazi et al., 2023, 2025). Each impact consistently triggered an early depolarisation that mirrored the injury potential documented in preclinical studies, with an amplitude proportional to the trauma intensity and modulated by varying extracellular ion concentrations. At the injury level, extensive cellular loss and disconnection of input along the spinal cord closely parallel severe clinical SCI conditions. Moreover, the hypotonia and areflexia characteristic of clinical spinal shocks were reproduced *ex vivo* by the suppression of spontaneous motor activity recorded from all ventral roots (VRs) and by transient failure of afferent pulses, reflecting the impairment of spinal synaptic transmission. However, the extent to which an injury potential affects the chances of functional recovery remains unclear. Additionally, we do not know how injury-induced depolarisations contribute to the cascade of neurotoxic events, known as secondary damage.

In the present study, we explored whether limiting post-injury depolarisation could promptly restore reflexes and protect neuronal networks via pharmacological manipulation of membrane receptors mediating fast ionic currents in the spinal cord. Besides the multiple neurotransmitter systems investigated so far to reactivate sensory motor networks following injury (Musienko et al., 2011), neurochemicals acting on ionotropic

Atiyeh Mohammadshirazi is a PhD graduate in Neurobiology from the International School for Advanced Studies (SISSA). Her doctoral research examined the immediate changes in CNS networks following spinal cord trauma. She also holds an MSc in Cellular and Developmental Biology from the Royan Institute for Stem Cell Biology and Technology, where her thesis focused on a combinational therapy using human pluripotent stem cell-derived neural stem cells in a rat model of spinal cord injury. Her wider research interests include neurophysiology, neuroregeneration and neurotrauma.

receptors implicated in the pathophysiology of acute SCIs might represent an optimal target to limit the sudden depolarisation following spinal trauma. In particular, low extracellular concentrations of chloride ions enhance the peak of injury potentials (Mohammadshirazi et al., 2025), reminiscent of the effect observed with low-chloride systemic perfusion on cortical spreading depression (Guedes & do Carmo, 1980). Hence, chloride-mediated fast inhibitory neurotransmission can be exploited by acting on both glycine and $GABA_A$ receptors. Furthermore, a massive surge of glutamate has been reported as an early consequence of an SCI (Liu et al., 1991; McAdoo et al., 1999, 2000; Xu, 2004), suggesting to reduce the early functional changes induced by the trauma by blocking ionotropic glutamate receptors already during the impact, using DL-2-amino-5-phosphonopentanoic acid (APV) and 6-cyano-7-nitroquinoxaline-2,3-dione disodium salt hydrate (CNQX), which mostly suppress spinal synaptic transmission (Bracci et al., 1996a; Mayer & Westbrook, 1987). Beyond ionotropic receptors, the wave of ions sustaining tissue depolarisation may propagate along the spinal cord via gap junctions. Indeed, gap junctions have been linked to axonal dysfunctions following SCI because their blockade by carbenoxolone limited impulse conduction loss (Goncharenko et al., 2014).

Moreover, microdialysis sampling at the injury site has revealed the acute release of adenosine (McAdoo et al., 2000), suggesting to limit the first consequences of a trauma by applying either adenosine, or the broad antagonist of adenosine receptors, caffeine, or more selectively, the A1 receptor blocker, 8-cyclopentyl-1,3-dipropylxanthine (DPCPX), which has been reported to modulate sensorimotor networks in the spinal cord (McAdoo et al., 2000; Taccola et al., 2020).

As a result of stretch forces produced on the membrane of spinal neurons at the injury epicentre, mechanoreceptors might also be involved in the trauma response. Mechanosensitive neurons express a broad class of mechanically gated ion channels, which are activated by shear forces on nearby membranes and are coupled to cations currents (Garcia-Elias et al., 2014). Although mechanoreceptors have been identified in spinal cord of lampreys (Grillner et al., 1982) and lizards (Alibardi, 2019), evidence for their presence in the ventral spinal cord of mammals remains limited.

Among the four superfamilies of mechanoreceptors (Valle et al., 2012), the transient receptor potential (TRP) family includes the transient receptor potential, vanilloid 4 (TRPV4), a calcium-permeable non-selective cation channel expressed by astrocytes and neurons, and distributed widely throughout the CNS, including in the adult spinal cord, although at relatively low levels (Kumar et al., 2020). However, TRPV4 expression in neonatal spinal cords has not yet been reported. Once activated, TRPV4 not only depolarises the cell membrane, but also modulates ligand-gated chloride channels, such as $GABA_A$ receptors and strychnine-sensitive GlyR (Hong et al., 2016; Qi et al., 2018). TRPV4 channels are activated by a broad range of stimuli because they function as osmoreceptors sensing mechanical stimulation from cell swelling, and as thermosensors responsive to temperatures above 27°C (Kumar & Han, 2022). Spinal cord injuries increase the expression of TRPV4 in proportion to trauma severity, and mostly during the early inflammatory phase that occurs from 1 to 8 h after SCI (Kumar & Han, 2022; Kumar et al., 2020). Genetic suppression of TRPV4 or intraperitoneal administration of the selective pharmacological TRPV4 antagonist 1 h after SCI, enhanced neuroprotection against SCI-induced endothelial damage with preserved blood-spinal cord barrier integrity, attenuated neuroinflammation and reduced glial scarring at the epicentre of injury, with some motor recovery in hindlimbs (Kumar et al., 2020). However, these observations were obtained in adults, leaving the issue of the pathophysiology of SCI in neonates unexplored.

Given the limited understanding of SCI mechanisms in neonates, we hypothesise that membrane pore-forming proteins, including mechanoreceptors, gap junctions and the ionotropic receptors examined in this study, are immediately activated upon impact. We further suppose that these proteins could sustain the extracellular ion imbalance underlying both, depolarising injury potentials (DIPs) and the transient suppression of motor reflex responses (MRRs) during the spinal shock. Our aim is to define a selective neonates-specific pharmacological strategy to block these membrane pores in order to limit the extent of injury potentials and accelerate the recovery of reflexes following the shock-like phase triggered by a physical trauma to the cord. To this end, in the present study, spinal impacts of equal severity were singularly performed on different preparations. Each preparation was then perfused with a single neuroactive drug before the impact and for the following recovery phase. Amplitude and latency of DIPs and time-courses of recovery of MRRs were compared with untreated injured cords. This study may explain the crucial roles played by mechanosensitive TRPV4 receptors, as well as other membrane pores, in the pathophysiology of an acute spinal trauma, suggesting potential implications for a clinical translation aimed at limiting accidental damages to the cord during complicated deliveries (Vialle et al., 2008).

Methods

To explore the pharmacological modulation of the immediate consequences of a traumatic injury to spinal

cord, we adopted the *ex vivo* preparation of the entire CNS isolated from neonatal rats (Apicella & Taccola, 2023; Mohammadshirazi et al., 2023) with intact dorsal laminae (Mohammadshirazi et al., 2025). Continuous nerve recordings were performed from L5 ventral root (VRrL5), whereas sacrocaudal afferents were electrically stimulated at low frequency throughout the experiment (Fig. 1*A*). A calibrated severe impact was provided to the ventral side of the tenth segment of the thoracic spinal cord (T10).

Ethical approval

All procedures involving animals were approved by the International School for Advanced Studies (SISSA) ethics committee and were conducted in accordance with the guidelines of the National Institutes of Health (NIH) and the Italian Animal Welfare Act 24/3/2014 n. 26, implementing the European Union directive on animal experimentation (2010/63/EU). Every measure was taken to minimise the number of animals used and

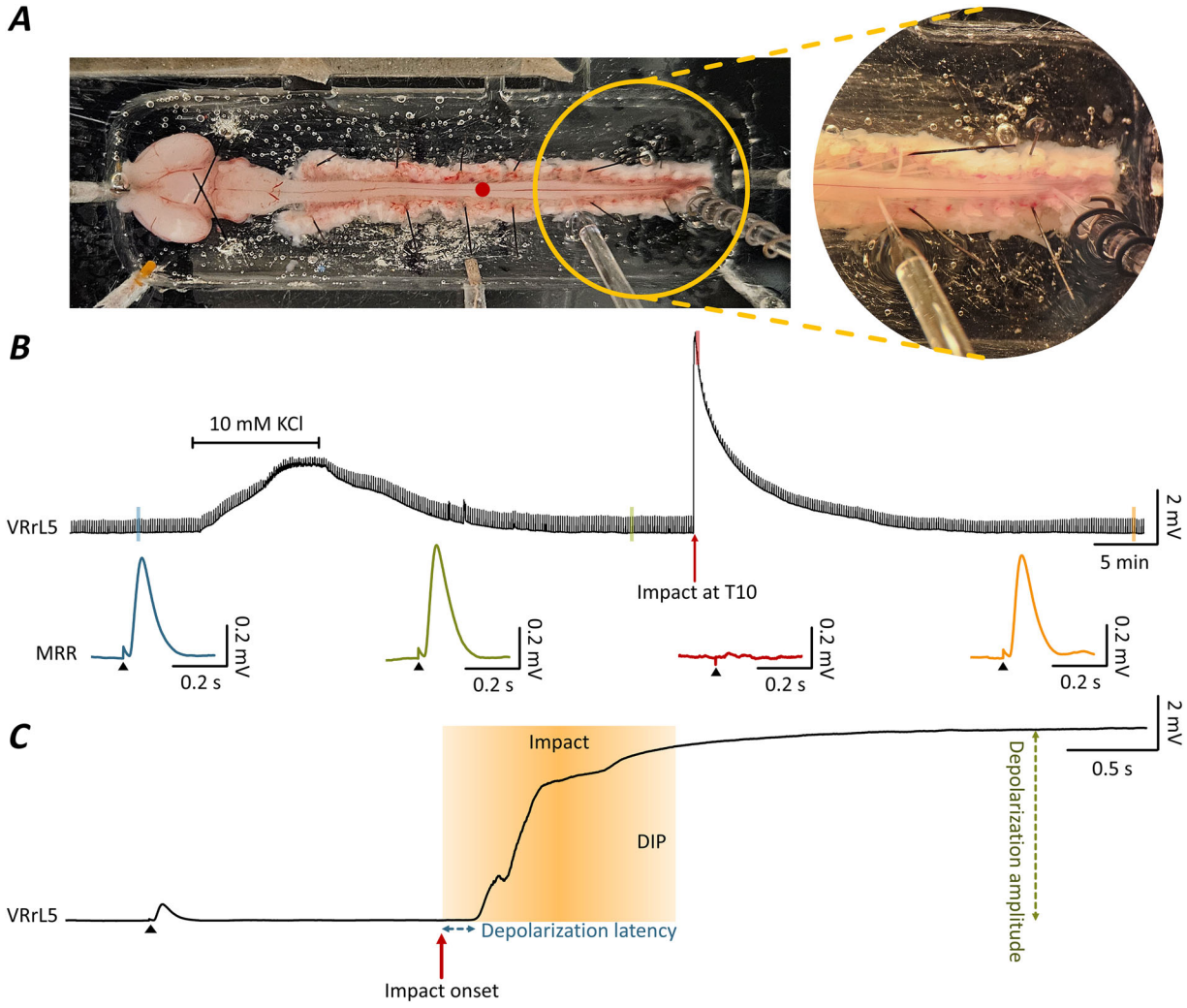

Figure 1. Transient depolarisation induced by a physical injury to the spinal cord in an *ex vivo* CNS preparation
A, image of the electrophysiological setup for *ex vivo* preparations of the entire CNS with intact dorsal aspects of vertebrae. Throughout the experiment, continuous recordings were derived from VRrL5, as electrical stimulation was applied to sacrocaudal afferents every 10 s. Physical impact was performed at T10 (red dot). *B*, a long continuous recording from VRrL5, when the cord was impacted at T10 (red arrow). Ten minutes of perfusion with 10 mM KCl represents an internal control to quantify the large recruitment of motor pools. Below: three examples of electrically induced motor reflex responses (MRR) are magnified before (blue) and after (green) KCl application, at the top of the injury potential (red) and once recovered from impact-induced depolarisation (orange). *C*, magnified 6 s trace extracted from (*B*) highlights the instants around the impact and defines latency (blue dotted arrow) and amplitude (green dotted arrow) of the depolarising injury potential (DIP). The pale orange field corresponds to the total duration of the spinal compression, from the lowering of the impactor to the full decompression (1.30 s). VRrL5, L5 ventral root.

to ensure their welfare. All procedures were carried out in compliance with the policies of *The Journal of Physiology* regarding animal experiments.

Ex vivo preparation of the entire CNS

Ex vivo preparations of the entire isolated CNS (Apicella & Taccola, 2023; Mohammadshirazi et al., 2023) coming from 111 postnatal (P0–P2.5) Wistar rats of both sexes were randomly selected in this study. Animals were obtained from the SISSA vivarium under the following authorisation numbers: n.36835 GEN.IV-1-J-A-1 (issued on 09/08/2010), U.Z.10/10-1/10-9 (issued on 28/09/2010) and subsequent authorisations Q 11/7/1-76/23/4-(3255) and 285421. Neonates were naturally fed by their mothers, who had *ad libitum* access to food and water under standard husbandry conditions.

Cryoanaesthesia was induced by placing the neonatal rat on a mat inside a pre–chilled chamber with an iced floor, ensuring that the animal did not come into direct contact with the ice. The animal remained in the chamber for 7–9 min, allowing its body temperature to decrease until anaesthesia was achieved, as indicated by the disappearance of the paw–pinch reflex (Danneman & Mandrell, 1997; Goldberg, 2015; Phifer & Terry, 1986). Under cryoanaesthesia, the animal was removed from the chamber and immediately killed by thoracotomy followed by cardiac ablation, in accordance with Allegato VI describing authorised procedures for organ collection (project code 22DAB.N.AHH), as approved by the Italian Ministry of Health on 23/12/2024.

Following death, quick surgical procedures were performed, including removal of forehead at orbital line, rib cage, internal organs and forelimbs. Dissection continued under the microscope in a Petri dish filled with an oxygenated Krebs solution that contained (in mM): 113 NaCl, 4.5 KCl, 1 $MgCl_2{\cdot}7H_2O$, 2 $CaCl_2$, 1 NaH_2PO_4, 25 $NaHCO_3$ and 30 glucose, gassed with 95% O_2–5% CO_2, pH 7.4, 299.62 ± 3.2 mOsm kg^{-1}. Craniotomy and ventral laminectomy were then performed, keeping dorsal vertebra and dorsal root ganglia (DRG) intact (Mohammadshirazi et al., 2025) and the preparation was maintained in the oxygenated Krebs solution at room temperature for 15 min and thus transferred to the recording chamber with perfusing oxygenated Krebs solution (7 mL min^{-1}) and controlled temperature of 25–27°C (TC-324; Warner Instruments, Holliston, MA, USA). For electrophysiological recordings, the preparation was fixed ventral side up and selected VRs were detached from DRGs.

Extracellular recordings

Monopolar suction electrodes were created by pulling tight-fitting glass pipettes (1.5 mm outer diameter, 0.225 mm wall thickness; Hilgenberg, Malsfeld, Germany) and used to obtain DC-coupled recordings from VRrL5. Electrodes were connected to a differential amplifier (DP-304; Warner Instruments), and signals were acquired with ×1000 gain, 0.1 Hz high-pass and 10 kHz low-pass filter. After noise elimination of analogue signals (D400; Digitimer Ltd, Welwyn Garden City, UK), traces were digitised with a sampling rate of 5 kHz and low-pass filtrated at 10 Hz (Digidata 1440; Molecular Devices Corporation, Downingtown, PA, USA; digital Bessel) and visualised real-time (software Clampex 10.7; Molecular Devices Corporation).

Electrical stimulation

A programmable stimulator (STG4002; Multichannel System, Reutlingen, Germany) and bipolar glass suction electrodes connected to two paired silver wires (500–300 μm) were utilised to produce electrical stimulations. Trains of rectangular electrical pulses of 40–160 μA intensity, 0.1 ms pulse duration and 0.1 Hz frequency were supplied to the *cauda equina* (Etlin et al., 2010). Stimulus intensity was imputed as times to threshold (Th), which is defined as the lowest intensity required to elicit a slight deflection of VRrL5 baseline.

Spinal cord injury

A custom-made and shielded micro-impactor device was used to provide traumatic damage to the spinal cord of the entire CNS *ex vivo* (Mohammadshirazi et al., 2025).

A calibrated impact was applied to the ventral surface of thoracic 10 (T10) during which electrophysiological recordings were simultaneously performed. A dedicated software controlled the vertical movement of the impactor tip (diameter = 2 mm). To provide a severe damage to the spinal cord, the impactor tip descended quickly (compression time = 650 ms, total duration from the first compression to a full decompression = 1.30 s) into the cord by 2656 μm from the spinal surface (speed = 4 mm s^{-1}, acceleration and deceleration = 6.1 ± 0.05 mm s^{-1}) and promptly returned to the original position with the same acceleration and deceleration speed.

Pharmacology

Based on their solubility product constant (K_{sp}), powders of pharmacological agents were dissolved in a proper solvent to make concentrated stocks that were then serially diluted in oxygenated Krebs solution to reach the final concentration. All pharmacological agents were perfused into the recording chamber when the impact was being performed on the spinal cord. Concentration and time of application are mentioned in Table 1. All chemicals were

Table 1. Pharmacological agents applied in the study, final concentration, type of solvent and time of perfusion

Agents	Target of compounds	Concentration (μM)	Solvent	Time of application before impact (min)	Time of application after impact (min)
DL-2-Amino-5-phosphonopentanoic acid (APV)	NMDA receptors	100	Water	20	5
6-Cyano-7-nitroquinoxaline-2,3-dione disodium salt hydrate (CNQX)	AMPA/kainate receptors	20	DMSO	20	5
Carbenoxolone disodium (CBX)	Gap junctions	100	Water	50	5
Adenosine (ADO)	adenosine receptors	1000	Krebs	5	15
Caffeine	A1 and A2A adenosine receptors	300	Water	15	5
8-Cyclopentyl-1,3-dipropylxanthine (DPCPX)	A1 adenosine receptors	5	Sodium hydroxide	5	5
AP-18	TRPA1 channels	20, 50, 66	DMSO	15	5
RN-1734	TRPV4 channels	10, 20, 50, 100	DMSO	15	5
Glycine (Gly)	Glycine receptors	500	Krebs	20	5
1(*S*),9(*R*)-(−)-bicuculline methiodide (bic)	$GABA_A$ receptors	20	Water	20	10
Strychnine (str)	Glycine receptors	1	Water	20	10

purchased from Sigma-Aldrich (Merk Life Science S.r.l., Milan, Italy).

Immunostaining

We adapted a published immunofluorescence protocol for the immunofluorescence staining experiments (Ciani et al., 2023). Seventeen spinal cords from neonatal rats (P0–P2) were embedded in OCT and were cryosectioned (Cryotome FE & FSE; A78910100; Thermo Fisher Scientific, Waltham, MA, USA) into 20 μm slides and collected on SuperFrost Plus Adhesion slides (#10149870; Thermo Fisher Scientific) and stored at −80°C until staining. Each slice was boiled in sodium citrate 10 mM antigen retrieval buffer for 5 min, and then incubated in 0.1% Sudan Black for 30 min, followed by a quick wash in ethanol 70%, another quick wash in ethanol 50% and a final wash in phosphate-buffered saline (PBS) for 4 min. Slices were blocked in 10% donkey serum solution for 1 h at room temperature, and then incubated overnight with the following primary antibodies diluted in 1:5 blocking solution: anti-glial fibrillary acidic protein (GFAP) chicken (dilution 1:500; catalog. no. PA1-10004; RRID:AB_1074620; Invitrogen, Waltham, MA, USA); anti-TRPV4 rabbit (dilution 1:300; catalog. no. ab39260; RRID:AB_1143677; Abcam, Cambridge, UK); and anti-NeuN mouse (dilution 1:250; catalog. no. MAB377; RRID:AB_2298772; Millipore, Burlington, MA, USA).

The next day, slices were washed in PBS 1 × three times for 10 min each and then incubated for 2 h at room temperature with the following secondary antibodies, followed by three washes in PBS (10 min each): donkey anti-mouse IgG (H+L) highly cross-adsorbed secondary antibody, Alexa Fluor 594 (dilution 1:400; catalog. no. A-21203; RRID:AB_141633; Invitrogen); donkey anti-rabbit IgG (H+L) highly cross-adsorbed secondary antibody, Alexa Fluor 488 (dilution 1:400; catalog. no. A-21206; RRID:AB_141633; Invitrogen); donkey anti-chicken IgG(H+L) highly cross-adsorbed secondary antibody, Alexa Fluor 647 (dilution 1:1000; catalog. no. A78951; RRID:AB_2921073; Thermo Fisher Scientific).

For nuclear staining, samples were incubated with 4′,6-diamidino-2-phenylindole (DAPI; dilution 1:1000; 32670; Merck-Sigma, St Louis, MO, USA) in 1 × PBS for 5 min at room temperature and then washed three times for 10 min each with 1 × PBS. The cover slips were then mounted, sealed with Fluoromount-GTM (00-4958-02; Invitrogen) and allowed to dry at room temperature in a dark container.

Imaging

An A1/R confocal microscope (Nikon, Tokyo, Japan) was used to take high-resolution images with 20× and 100×

oil objectives. To include all the cells across the whole tissue thickness, images were taken as follows: for the large panoramic images at 20×, as z-stacks of at least 11 steps of 2 μm, including an optical section thickness of at least 20 μm; for the single images at 100×, the z-stacks were of 21 steps of 1 μm each, to reach always a final optical section thickness of 20 μm. Images were subsequently processed as z-stack MAX-projection modality in FIJI software (ImageJ, Bethesda, MD, USA).

Statistical analysis

Data analysis was pursued using Clampfit, version 10.7 (Molecular Devices Corporation), and statistical analysis was performed with InStat 3.10 (GraphPad Software Inc., San Diego, CA, USA). The number of animals is indicated as '*n*' and data are reported as the mean ± SD. The latency is defined as the time spanning from either the electrical stimulation or the mechanical artefact to the onset of increased DC level. Time to peak refers to the temporal delay from the artefact of stimulation to the peak of the subsequent evoked response. Power spectrum analysis was carried out generate a frequency domain representation, revealing the power levels of different frequency components in the signal. Bursting activity was quantified in terms of power spectrum magnitude, expressed as root mean square (RMS) (Deumens et al., 2013) and measured with Clampex, version 10.7 (Molecular Devices Corporation). This statistical tool quantifies any increase in frequency and/or amplitude of rhythmic activity, defined as a complex rhythm composed of multiple harmonics. Prior to any other statistical tests, a normality test was performed. Parametric paired Student's *t* test or non-parametric Wilcoxon matched pairs test, or the Kruskal–Wallis test following Dunn's multiple comparisons to control data, were utilised. $P < 0.05$ was considered statistically significant. Data distributions were visualised using box plots generated in Excel (Microsoft Corp., Redmond, WA, USA). The box plots display the interquartile range (IQR), with the lower and upper bounds of the box representing the first (Q1) and third quartiles (Q3), respectively. The line inside the box shows the inclusive median, and the mean value is marked by a cross. Whiskers extend to the most extreme data points that are within 1.5 times the IQR from the box's edges, whereas any outliers beyond this range are plotted individually as dots.

Results

A traumatic injury to the spinal cord generates a large, transient injury potential

In a representative experiment, the impact induced an early depolarisation that started after only 186.44 ms after contact with the impactor, peaked at 7.14 mV after 5.42 s after mechanical force application (Fig. 1*B* and *C*), and recovered back to baseline within ∼25 min. In 12 preparations, the same traumatic injury generated a sudden DIP with a latency of 188.62 ± 8.70 ms that reached a maximal mean amplitude of 5.50 ± 2.84 mV after 2.13 ± 1.26 s, and recovered to baseline in 11.99 ± 8.93 min.

Next, we compared DIPs with depolarisations induced by the standard depolarising solution containing 10 mM KCl. A 10 min perfusion with a K^+ physiological solution (10 mM) depolarised VRs by 2.57 ± 1.09 mV ($n = 12$). In the same experiments, the mean amplitude of the DIP in physiological solution was more than double (226.79 ± 121.63%, $n = 12$) than the depolarisation elicited by potassium.

To monitor the impact of trauma on motor output, in a sample experiment, a train of electrical pulses (0.1 ms pulse duration, 0.1 Hz frequency, 160 μA intensity) was continuously applied to sacrocaudal afferents (Fig. 1*B*) and induced, in control, an MRR of 0.49 mV amplitude, which diminished at the peak of the potassium-induced depolarisation (29.92% of control) with a full recovery (101.12% of control) in 2.70 min after injury. Conversely, MRRs totally disappeared at the peak of the injury-induced potential, with a substantial recovery (80.79% of control) (Fig. 1*B*) after 36.33 min from injury. Noteworthy, recovery of MRRs after both, chemically and mechanically induced depolarisations, confirms that neither a perfusion with 10 mM KCl nor a severe impact at T10 reduced functionality of lumbar motor pools (Fig. 1*B*). In six experiments, trains of stimuli (60–160 μA intensity) evoked mean MRRs of 0.82 ± 0.25 mV amplitude in control, which were largely reduced at the peak of the potassium-induced depolarisation (0.21 ± 0.19 mV) with a full recovery (96.86% ± 2.86%) after 7.76 ± 3.68 min of washing. Moreover, mean MRRs were completely suppressed at the peak of the injury-induced potential, with a substantial recovery to baseline values after 18.49 ± 10.21 min from injury ($n = 6$).

Effects of traumatic injury over baseline activity and MRRs

To modulate the extent of depolarisation and the suppression of MRRs after injury, in separate experiments, selected neurochemicals implicated in the pathophysiology of acute SCIs were perfused (Table 1) and their effects on baseline activity were traced before injury.

First, we explored the role of glutamate signalling using the antagonists of inotropic glutamate receptors, APV (100 μM) + CNQX (20 μM), which slightly polarised

the DC level, reaching a peak of 0.29 ± 0.10 mV ($n = 5$) after 7.45 ± 2.20 min perfusion and remaining stable thereafter. With APV + CNQX, MRRs gradually decreased, reaching 20% of their original value in amplitude within 5.39 ± 1.25 min, and completely disappeared after 8.31 ± 1.77 min ($n = 5$). Adenosine (1 mM) polarised baseline by 0.34 ± 0.12 mV after 4.21 ± 0.59 min ($n = 6$), but also reduced and delayed MRRs (amplitude: $P = 0.003$, time to peak: $P = 0.041$, paired *t* test) (Table 2). Caffeine (300 μM), a non-specific adenosine receptor antagonist, did not affect DC levels, but increased the latency of MRRs ($P = 0.039$, paired *t* test) (Table 2). Following glycine (500 μM) application, a small depolarisation of 1.70 ± 0.66 mV ($n = 6$) occurred within 2.31 ± 0.42 min. Within 6.06 ± 2.46 min, a spontaneous repolarisation occurred, settling the baseline at 0.88 ± 0.33 mV above the original DC level, whereas amplitude of MRRs decreased significantly ($P < 0.001$, paired *t* test) (Table 2). Application of the $GABA_A$ receptor antagonist, bicuculline (20 μM), depolarised the baseline by 2.60 ± 0.75 mV within 4.02 ± 0.49 min ($n = 4$), which repolarised to baseline (0.16 ± 0.17 mV) after 7.16 ± 1.83 min of continuous application of bicuculline, accompanied by rhythmic bursting (Bracci et al., 1997). Spectral analysis was performed on 5 min segments of traces recorded in bicuculline at steady-state. The resulting mean RMS value was 8.68 times greater than the RMS calculated from baseline spontaneous activity in control, mirroring the appearance of a rhythmic activity (from 0.10 ± 0.05 in control to 0.83 ± 0.38 during bicuculline; $P < 0.001$, paired *t* test, $n = 11$). Also, application of the glycinergic receptor antagonist, strychnine (str) (1 μM), induced bursting activity (Bracci et al., 1996b) with a mean RMS value 2.58 times higher than the one calculated for baseline spontaneous activity in control before str application (from 0.13 ± 0.09 to 0.34 ± 0.2; $P = 0.031$, paired *t* test, $n = 5$). Finally, when bicuculline (20 μM) and strychnine (1 μM) were co-applied, baseline depolarised on average by 2.97 ± 0.99 mV within 4.11 ± 0.84 min from application of drugs and then spontaneously ripolarised to original baseline values within 6.22 ± 0.91 min of continuous application of bic + str ($n = 12$). Appearance of disinhibited bursting (Bracci et al., 1997) corresponds to an 8.46-fold increase in mean RMS compared to pre-drug applications (from 0.12 ± 0.15 mV in control to 1.03 ± 0.27 mV in str + bic; $P < 0.001$, paired *t* test, $n = 7$). Application of the gap junction blocker, carbenoxolone (CBX) (100 μM), the selective antagonist for adenosine A1 receptors, DPCPX (5 μM), the TRPA1 channel blocker, AP-18 (20, 50 and 66 μM) or the TRPV4 channel antagonist, RN1734 (10, 20, 50 and 100 μM) did not significantly alter DC levels nor MRRs. Detailed changes in MRR amplitude, as well as time to peak

Table 2. Amplitude and time to peak of MRRs, with statistical comparisons before and after the application of each pharmacological agent

Agents	*n*	MRR parameter	Before application	After affection of the drug	Test	*P* value
CBX	5	Amplitude (mV)	0.33 ± 19	0.28 ± 0.16	Paired *t* test	0.180
	7	Time to peak (ms)	75.82 ± 6.63	78.07 ± 4.50	Paired *t* test	0.281
ADO	6	Amplitude (mV)	1.11 ± 0.46	0.55 ± 0.26	Paired *t* test	0.003
	6	Time to peak (ms)	75.67 ± 5.41	71.62 ± 3.58	Paired *t* test	0.041
Caffeine	5	Amplitude (mV)	0.85 ± 0.47	0.80 ± 0.51	Wilcoxon matched pairs test	0.313
	5	Time to peak (ms)	77.06 ± 5.13	80.05 ± 5.10	Paired *t* test	0.039
DPCPX	5	Amplitude (mV)	0.40 ± 0.13	0.78 ± 0.68	Wilcoxon matched pairs test	0.813
	5	Time to peak (ms)	78.36 ± 4.81	78.17 ± 5.80	Paired *t* test	0.800
RN1734	4	Amplitude (mV)	0.42 ± 0.23	0.34 ± 0.21	Wilcoxon matched pairs test	0.25
	4	Time to peak (ms)	79.83 ± 4.05	86.68 ± 6.12	Wilcoxon matched pairs test	0.125
Gly	6	Amplitude (mV)	0.62 ± 0.22	0.38 ± 0.18	Paired *t* test	0.0003
	6	Time to peak (ms)	80.93 ± 3.93	79.3 ± 2.32	Paired *t* test	0.119
Str	5	Amplitude (mV)	0.60 ± 0.17	0.90 ± 0.35	Wilcoxon matched pairs test	0.125
	5	Time to peak (ms)	76.12 ± 6.66	82.57 ± 7.78	Paired *t* test	0.101

'*n*' indicates the number of experiments in each group, with each experiment represented by the average of five data points.

values and associated statistical analyses, are provided in Table 2.

Basal expression of mechanoreceptors in the spinal cord and their changes after injury

To determine the cellular location of the TRPV4 marker, we performed co-immunostaining sections of uninjured spinal cords using antibodies against TRPV4, NeuN and GFAP. Tissue samples were obtained from two separate control preparations and processed for both sagittal (Fig. 2*A*–*E*) and coronal sections at the T10 level (Fig. 2*F*–*J*). We observed that TRPV4 staining is uniformly distributed along the thoracic spinal cord (Fig. 2*E*). Notably, TRPV4 is mainly localised around the central canal, at the borders of the spinal cord, and throughout the grey matter. Both small dorsal neurons and larger ventral cells in lamina IX, putatively motoneurons, were positive for the staining (Fig. 2*J*). Indeed, the colocalisation of TRPV4 with NeuN confirmed strong expression of this mechanoreceptor in neuronal cell body. Also, we found that TRPV4 is consistently localised in correspondence to glia limitans, with clear colocalisation with GFAP, indicating TRPV4 expression in astrocytes as well. Similar patterns were reported in four additional intact spinal cords from *ex vivo* CNS preparations spanning from P0 to P2. In a sperate series of 11 preparations, TRPV4 immunolabelling was assessed at different time points (25 min, 1 h and 2.5 h) following an impact to the T10 segment. TRPV4 expression in the thoracic cord around the lesion site remained unchanged at all assessed time points (see Appendix, Fig. A1).

Pharmacological manipulation of the peak of DIPs

All pharmachological agents used have been applied in the recording bath in the exact moment when physical injury was produced to the thoracic segment (T10) of the spinal cord. Concentrations, as well as timing of application, were defined as time values before and after the impact (Table 1). The DC level of baseline was continuously recorded from VRrL5. The peak of DIP was normalised to that previously elicited by the application of a 10 mM potassium medium in the same experiments (Fig. 3*A*). Among all drugs tested, only RN1734 at concentrations greater than 50 μM significantly reduced, on average, the normalised amplitude of DIPs by 35.25% compared to control untreated preparations ($P = 0.034$, Kruskal–Wallis test followed by Dunn's multiple comparisons test) (Fig. 3*B*). However, no significant differences were observed in the onset of DIPs in response to the application of any of the drugs tested ($P = 0.522$, Kruskal–Wallis test followed by Dunn's multiple comparisons test). In summary, DIP was smaller when RN1734 was perfused to the preparation during impact.

Pharmacological manipulation of MRRs

Dynamics of the recovery of MRRs following injury varied with each drug tested (Fig. 4*A*). The amplitude of MRRs was normalised to pre-impact values for each preparation. Two time-points were considered. In untreated injured preparations, a slow spontaneous recovery in the peak of MRRs occurred after injury, reaching 28.97% ± 17.17% of pre-impact after 1 min and 45.64% ± 28.05% after 2 min. Conversely, in preparations treated with CBX, MRRs partially recovered to 66.39% ± 19.32% of pre-impact control values immediately after the impact (1 min). At the same time point, RN1734 completely restored pre-impact MRRs (90.70% ± 28.48%). Both CBX and RN1734 significantly improved the amplitude of normalised MRRs 1 min after impact compared to the peak of normalised MRRs in untreated spinal cords ($P = 0.004$, Kruskal–Wallis test followed by Dunn's multiple comparisons test) (Fig. 4*B*). With a longer delay from the trauma (2 min), bic also brought a full recovery of normalised MRR amplitude values (90.12% ± 22.14% of pre-impact) ($P = 0.018$, Kruskal–Wallis test followed by Dunn's multiple comparisons test) (Fig. 3*C*). Moreover, no significant difference was observed in the rate of MRR recovery following application of any of the other drugs tested at either time points. Collectively, after a physical trauma to the spinal cord, CBX speeded up the early partial recovery of MRRs, whereas both RN1734 and bic stably restored full MRRs, even with a temporal profile that makes RN1734 more effective than bic.

Discussion

The main findings of the present study indicate a key role of TRPV4 mechanosensitive receptors in the pathological sequelae of neonatal spinal trauma, measured as DIP amplitude and subsequent MRR recovery. Interestingly, GABAergic signalling and gap junctions were selectively involved in the recovery process, indicating that DIP and MRR events can be modulated independently. Given the widespread distribution of TRPV4 receptors in neurons, vessels and glial cells, our study suggests that these mechanosensitive receptors are a potential pharmacological target to ameliorate the pathological consequences of SCI.

Pathophysiology of DIP

Recently, we described a novel phenomenon of DIP presented that a massive transient depolarisation induced by acute mechanical injury quickly applied to the spinal

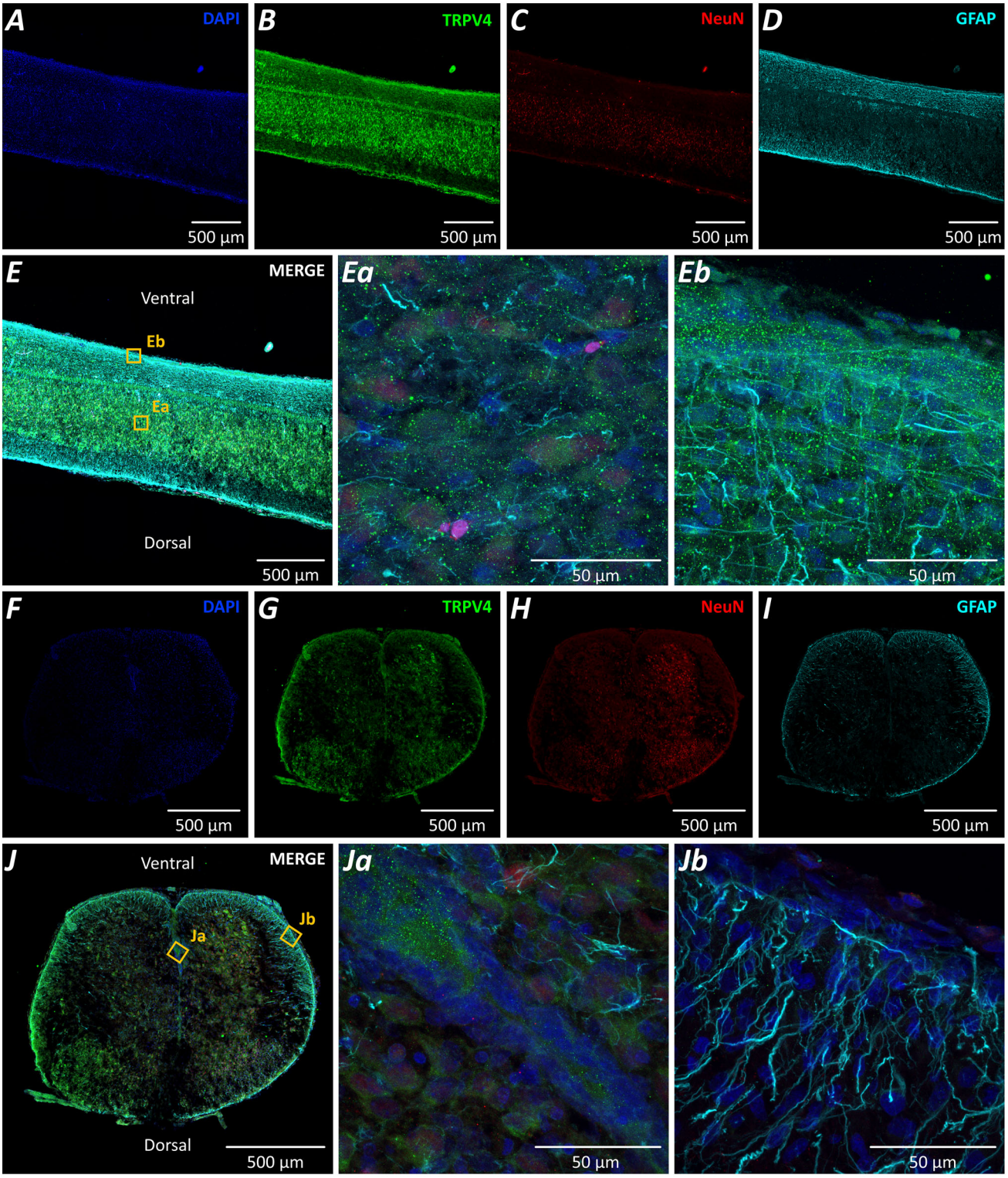

Figure 2. TRPV4 receptors are labelled in spinal neurons and astrocytes
Large images of the spinal cord in sagittal view (*A–D*) and cross-section view (*F–I*) immunostained for DAPI (in blue), TRPV4 (in green), NeuN (in red) and GFAP (in cyan). Merged images stained with immunofluorescence for TRPV4, NeuN and GFAP are visible in (*E*) and (*J*). Ventro-dorso polarity of the cord is reported. Scale bars = 500 µm. ***Ea*** and ***Eb***, Magnifications (100×) of the representative spinal cord sagittal section in (*E*) at the level of the central canal (***Ea***) and glia limitans (***Eb***). Scale bars = 50 µm. ***Ja*** and ***Jb***, Magnifications (100×) of the representative spinal cord coronal sections in (***J***) at the level of the central canal (***Ja***) and glia limitans (***Jb***). Scale bars = 50 µm. In all

panels, DAPI is visualised in blue, TRPV4 in green, NeuN in red and GFAP in cyan. Sagittal and coronal sections were collected from two different intact spinal cords from entire CNS preparations isolated from a P2.5 and a P0 animal, respectively. DAPI, 4′,6-diamidino-2-phenylindole; TRPV4, transient receptor potential, vanilloid 4.

cord (Mohammadshirazi et al., 2025). In this study, our continuous recording of MRR before and after trauma allowed us to monitor in very detail the dynamic of MRR disappearance and their progressive recovery. Thus, these testing events were slightly sensitive to the prior depolarisation induced by mild depolarisation induced by 10 mM KCl and almost completely disappeared during DIP. Both the amplitude of DIP and the time course of subsequent recovery served as a versatile protocol for testing various biological active compounds as potential treatments for reducing outcome of the SCI.

The nature of the novel DIP phenomenon remains not fully understood. However, the efficiency of the TRPV4 blocker in reduction of DIP amplitude suggest the key role of mechanosensitive TRPV4 receptors as the main contributor to massive depolarisation. This is not unexpected given that these receptors coupled to non-selective cationic channels are highly sensitive to mechanical forces (Kumar & Han, 2022).

Apart from measurement of DIP amplitude, we also evaluated the conduction of DIP along the spinal cord. We previously found that DIP, which had higher values in segments closer to the site of injury, then spread both rostrally and caudally partiality losing its amplitude, at the speed of 0.03 ± 0.01 m s^{-1} (Mohammadshirazi et al., 2025). Such a speed of DIP propagation was much faster than the phenomenon of cortical spreading depolarisation (CSD speed of 3–5 mm min^{-1}; Leao, 1944). CSD is also presented as a wave of initial massive depolarisation followed by depression phase, which can also be induced in the cortex of adult animals by a mechanical trigger such as pin prick (Zhang et al., 2010) or after traumatic brain injury (TBI) (Best et al., 2025). Notably, CSD can be suppressed by the blockers of NMDA receptors (Somjen, 2001; Shatillo et al., 2015), whereas conduction of DIP along the spinal cord was not halted by blockers of ionotropic glutamate receptors, which act by suppressing the main spinal synaptic transmission.

Thus, despite the general similarity with CSD, DIP has its own specific characteristics; in particular, an unchanged degree of depolarisation when our preparation was exposed to glutamatergic antagonists. Such independence from glutamatergic signalling suggests that the conduction of DIP is not based on synaptic

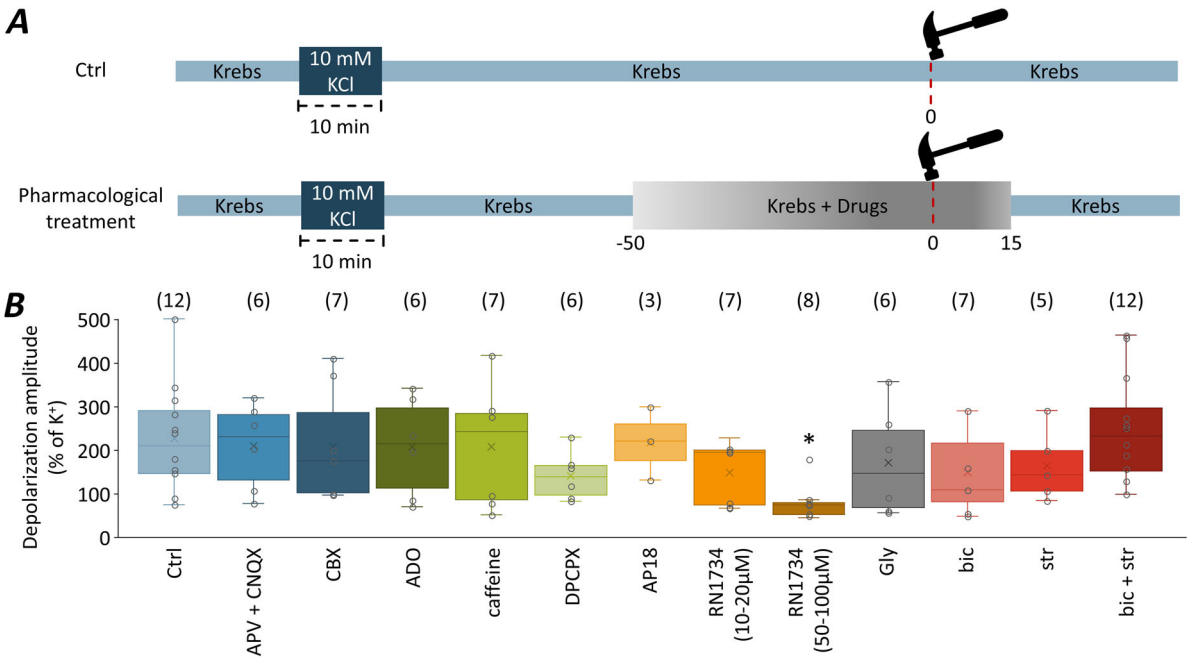

Figure 3. Amplitude of DIPs is reduced by TRPV4 antagonism
A, box-and-whisker plots schematise the experimental protocols used for impacts on untreated preparations (ctrl, above) and during perfusion with neurochemicals (drugs, below). *B*, bar graph displaying the normalised amplitude of DIPs recorded from VRrL5 during the impact in the presence of different pharmacological agents. Values are normalised as percentages of potassium-induced depolarisations in the same preparation (*$P = 0.034$). Total number of experiments in each group is indicated above each box. DIP, depolarising injury potential; TRPV4, transient receptor potential, vanilloid 4; VRrL5, L5 ventral root.

transmission and subsequent regenerative action potentials. By contrast, the delayed extrasynaptic volume transmission (Taber & Hurley, 2014) through the extracellular space and the spinal canal (Agnati et al., 2010) would better account for the more passive conduction of ions such as potassium, which is known to be released during neuronal depolarisation. In addition, the reduced peaks of injury potentials in response to the selective antagonism of mechanoreceptors are in accordance with a more passive flow of ions through pores opened during membrane stretching. Inevitably, ion movement results in osmotic changes in the extracellular fluid, leading to cell swelling and extracellular space shrinkage, hence sustaining the CSD (Guedes & do Carmo, 1980).

Pharmacology of DIP and MRR

Collectively, the physical impact to the neonatal spinal cord produced DIP and suppressed MRR, yet with a substantial recovery in the following 30 min. By measuring recovery of MRR in the presence of various pharmacological drug candidates, we found rather distinct rates of recovery from areflexia right after SCI.

The effect that distinct drugs have on the amplitude of DIP and the time required by the MRR to reappear unveils complex dynamics during and after the shock. Unexpectedly, glutamatergic, adenosinergic, glycinergic or GABAergic receptors were not implicated in sustaining the peak of DIP that follow a physical trauma to the spinal cord. However, the selective TRPV4 antagonist, RN1734, unlike the TRPA1 antagonist, AP18, limited the immediate consequences of the impact when perfused during compression. Moreover, blockage of gap junctions with CBX speeded up the reappearance of MRR, which only partially recover, whereas the antagonism of $GABA_A$ receptors with the GABAA antagonist bicuculline fully restored reflexes, although slightly later. The inhibitory action of TRPV4 blockade is consistent with alleviation of brain injury observed in the model of TBI (Michinaga, 2024).

The different recovery time obtained with the three agents may suggest a three-component mechanism at the base of the transient silencing of synaptic activity after trauma. In the first 6 s of an injury-induced depolarisation, the massive excitation appears to suppress MRR probably

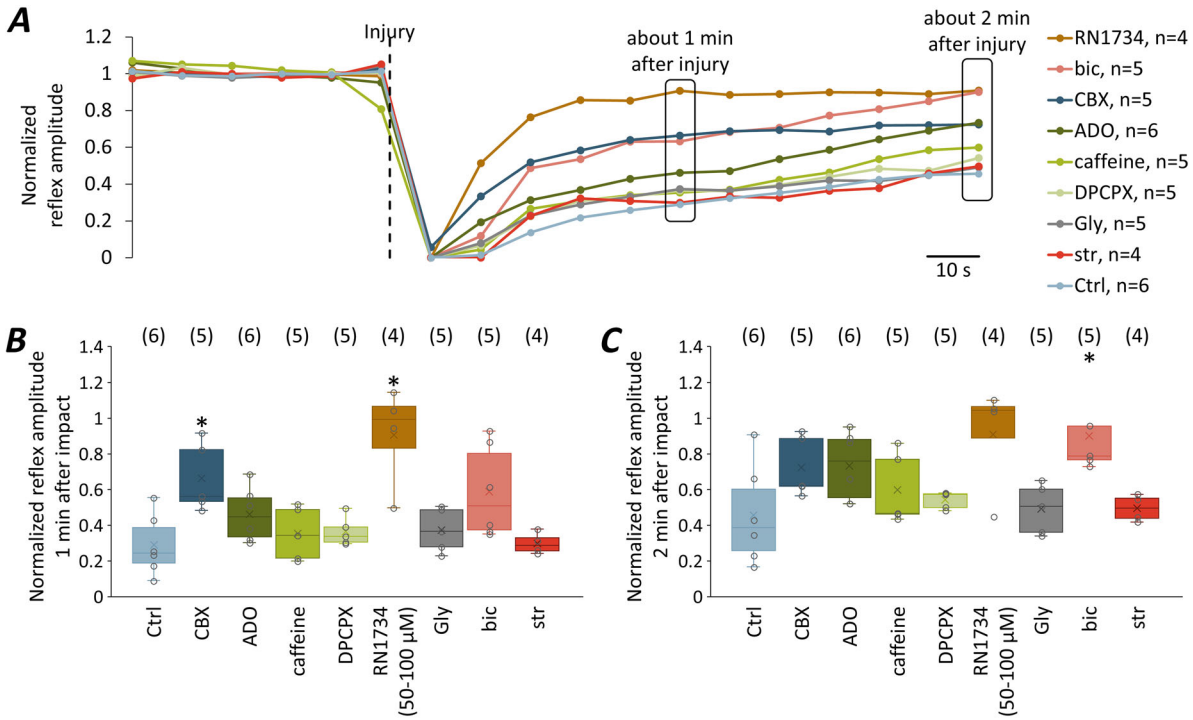

Figure 4. MRRs after a physical impact to the spinal cord recover with different rates depending on drug exposures
A, time courses of 3 min bins representing MRR amplitude recorded from VRrL5 after exposure to different drugs. Values are normalised to the average MRRs before the impact (indicated by the dotted line). The number of experiments is indicated as *n*. *B*, box-and-whisker plots illustrate normalised MRRs 1 min after the impact, corresponding to the left square in (*A*) (*P = 0.004). *C*, normalised MRRs 2 min after the impact, corresponding to the right square in (*A*) (*P = 0.018). The total number of experiments in each group is indicated above each box. MRR, motor reflex response; VRrL5, L5 ventral root.

as a result of the inactivation of voltage-gated sodium channels. This first massive depolarisation, albeit followed by a partial repolarisation, may sustain the following phase, lasting for up to 1 min after the impact, where gap junctions may be activated by their sensitivity to trans-junctional voltage (Stein et al., 2022). Sustained inward currents flowing through junction pores that are permeable to cations keep excitable cells inactivated for a longer period. Because gap junctions could be implicated in release of ATP (Cotrina et al., 2000), this early component of MRR recovery might be delayed as a result of the depolarising action of extracellular ATP on neurons or glial cells, which express a plethora of ATP-gated P2X receptors (Fields & Stevens, 2000).

The later recovery may have been a result of the latency caused by GABA release and action on target cells because it was sensitive to the GABA-A blocker bicuculline. This inhibitor input eventually reduces motor reflexes in the third phase of depolarisation, ∼2 min after trauma.

Widespread expression of TRPV4 mechanoreceptors contributing to injury-induced depolarisation

Given that selective blockade of mechanosensitive TRPV4 receptors reduces the extent of DIP, we specifically investigated the expression of these receptors in our model. Although mechanoreceptive neurons are not fully mature until 2 weeks postnatal (Jenkins & Lumpkin, 2017), our findings show that neonatal neurons in thoracic spinal segments uniformly express TRPV4 mechanoreceptors already at birth, both in the ventral and dorsal horns. In addition, strong TRPV4 labelling was observed in glial cells surrounding the central canal and at the dura interface, consistent with prior reports of TRPV4 expression in glia (Kanju & Liedtke, 2016). Interestingly, immunostaining in the present study did not reveal prominent TRPV4 expression in dural meningeal cells. However, the presence of mechanoreceptors around the outer borders of the cord, close to subarachnoid spaces in central and vertebral canals, suggests a potential role for TRPV4 receptors in detecting mechanical forces acting on the cord tissue during physiological back movements, as well as in the instants of a traumatic insult. Interestingly, trigeminal afferents of cranial meninges that express TRPV4 receptors generating migraine headache when activated (Wei et al., 2011) also showed mechanosensing capabilities during normal locomotion of awake mice (Blaeser et al., 2022).

The ability of TRPV4 antagonism to restore spinal reflexes may be partly ascribed to its modulation of $GABA_A$ currents. This is supported by the delayed recovery of MRR following the application of bicuculline, a $GABA_A$ receptor antagonist, although this did not affect the peak of the injury potential. These results underscore that two main hallmarks of the spinal shock, the magnitude of the DIP and the duration of reflex suppression, are governed by distinct mechanisms.

Peculiarities of spinal trauma in neonatal period

The mechanisms of SCI, widely studied in adults, remain largely unexplored in neonates, despite the fact that this type of injury occurs in obstetrics during complicated deliveries (Vialle et al., 2008). The present study, performed on neonatal (P1–P3) spinal cord tissue, essentially fills this gap. Despite the primary importance for spinal cord physiology and pathophysiology and the translational significance for clinical neonatology, one important issue is to what extent these mechanisms can be extrapolated to adult SCI. Although its superior *ex vivo* viability and relatively small size of spinal cord provide significant technical advantages for high-precision electrophysiology and circuit-level manipulation, important limitations in terms of translational relevance for adult injuries should be mentioned.

Thus, the neonatal spinal cord differs fundamentally from the adult spinal cord in many aspects including neuronal maturity and plasticity, as well as the profile of glial and immune cells (Marques-Smith et al., 2016). Among other factors, the most striking difference is that GABAergic signalling is depolarising in the neonatal spinal cord as a result of high NKCC1 and low KCC2 expression, leading to elevated intracellular chloride (Ben-Ari, 2002; Cherubini et al., 1991; Delpire & Staley, 2014; Mazzone et al., 2021). Although similar shifts in chloride homeostasis occur after adult SCI (Boulenguez et al., 2010), they reflect maladaptive reprogramming rather than a neonatal-specific developmental state.

In addition to their intrinsic plasticity, neonatal spinal cords exhibit a markedly higher regenerative capacity compared to adults (Stewart et al., 2022; Wang et al., 2004). This enhanced potential for repair coincides with the incomplete maturation of descending supraspinal pathways (Clarac et al., 2004; Lakke, 1997), which may influence both the pattern and extent of functional recovery following injury. Moreover, the neonatal immune environment is developmentally immature, and the activation profiles of microglia and astrocytes in response to SCI differ substantially from the robust inflammatory cascade typically observed in adults (Sutherland et al., 2017). These developmental distinctions underscore the need for age-specific models and therapeutic strategies when investigating spinal cord repair mechanisms.

Regarding comparison of neonates and adults, another type of signalling that appears to be central in neonatal SCI is the involvement of TRPV4 receptors. Notably, the profile and expression level of the TRPV4 receptor can

vary significantly during development. Thus, TRPV4 is dynamically regulated in the spinal cord and, in adults, shows context-dependent roles in injury, inflammation and mechanical sensitivity (Alessandri-Haber et al., 2005). In adults, TRPV4 is expressed in neurons, astrocytes and microglia (Kanju & Liedtke, 2016). In the present study, we found that, in neonates, it is expressed not only in neurons, but also in astrocytes. In adults, the deletion of TRPV4 receptors from microglia did not affect repair of the spinal cord after injury (Mertens et al., 2025), although this does not exclude the role of neuronal and/or astroglial TRPV4 receptors. Detailed characterisation of the TRPV4 receptor expression profile at different developmental periods requires further research, which represents another limitation for the relevance of the observed beneficial effects of the TRPV4 blockage to the adult SCI.

Conclusions

In conclusion, our findings indicate that both the severity of an SCI in neonates and the multifaceted process of functional recovery are modifiable mechanisms. These outcomes can potentially be improved through targeted pharmacological strategies, with TRPV4 receptor blockade emerging as a particularly promising approach for acute intervention following SCI. The present results lay the groundwork for future studies involving the administration of TRPV4 antagonists at the time of injury in anaesthetised adult rats. Extending the observation period into the chronic phase will be essential to evaluate long-term functional recovery and to better define the translational potential of TRPV4-targeted therapies also for injuries, including for adult SCI.

Appendix

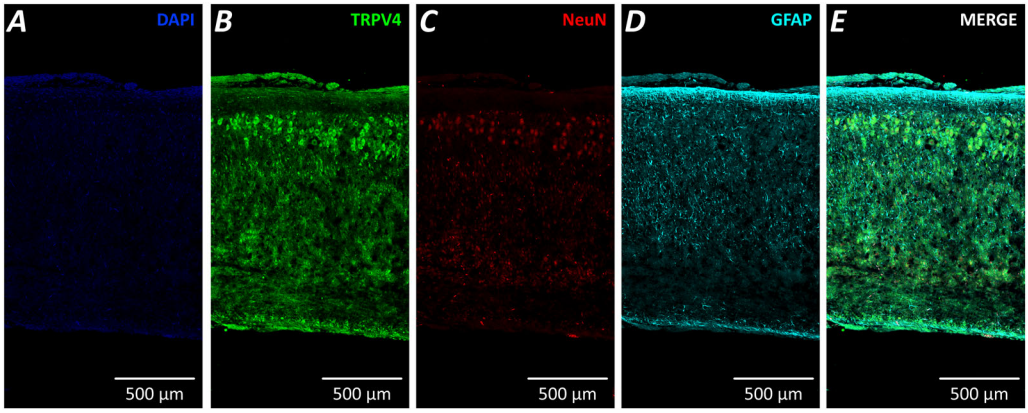

Figure A1.
Longitudinal sections of the thoracic spinal cord collected 25 minutes after impact, showing TRPV4 expression and immunolabeling for NeuN and GFAP.

References

Agnati, L. F., Guidolin, D., Guescini, M., Genedani, S., & Fuxe, K. (2010). Understanding wiring and volume transmission. *Brain Research Reviews*, **64**(1), 137–159.

Alessandri-Haber, N., Joseph, E., Dina, O. A., Liedtke, W., & Levine, J. D. (2005). TRPV4 mediates pain-related behavior induced by mild hypertonic stimuli in the presence of inflammatory mediator. *Pain*, **118**(1), 70–79.

Alibardi, L. (2019). Cerebrospinal fluid-contacting neurons in the regenerating spinal cord of lizards and amphibians are likely mechanoreceptors. *Journal of Morphology*, **280**(9), 1292–1308.

Apicella, R., & Taccola, G. (2023). Passive limb training modulates respiratory rhythmic bursts. *Scientific Reports*, **13**(1), 7226.

Ben-Ari, Y. (2002). Excitatory actions of GABA during development: The nature of the nurture. *Nature Reviews Neuroscience*, **3**(9), 728–739.

Best, F. V., Hartings, J. A., & Ngwenya, L. B. (2025). Repetitive cortical spreading depolarizations are prolonged early after experimental traumatic brain injury. *Experimental Neurology*, **385**, 115120.

Blaeser, A. S., Sugden, A. U., Zhao, J., Carneiro-Nascimento, S., Shipley, F. B., Carrié, H., Andermann, M. L., & Levy, D. (2022). Trigeminal afferents sense locomotion-related meningeal deformations. *Cell Reports*, **41**(7), 111648.

Boulenguez, P., Liabeuf, S., Bos, R., Bras, H., Jean-Xavier, C., Brocard, C., Stil, A., Darbon, P., Cattaert, D., Delpire, E., Marsala, M., & Vinay, L. (2010). Down-regulation of the potassium-chloride cotransporter KCC2 contributes to spasticity after spinal cord injury. *Nature Medicine*, **16**(3), 302–307.

Bracci, E., Ballerini, L., & Nistri, A. (1996a). Spontaneous rhythmic bursts induced by pharmacological block of inhibition in lumbar motoneurons of the neonatal rat spinal cord. *Journal of Neurophysiology*, **75**(2), 640–647.

Bracci, E., Ballerini, L., & Nistri, A. (1996b). Localization of rhythmogenic networks responsible for spontaneous bursts induced by strychnine and bicuculline in the rat isolated spinal cord. *Journal of Neuroscience*, **16**(21), 7063–7076.

Bracci, E., Beato, M., & Nistri, A. (1997). Afferent inputs modulate the activity of a rhythmic burst generator in the rat disinhibited spinal cord in vitro. *Journal of Neurophysiology*, **77**(6), 3157–3167.

Cherubini, E., Gaiarsa, J. L., & Ben-Ari, Y. (1991). GABA: An excitatory transmitter in early postnatal life. *Trends in Neuroscience (Tins)*, **14**(12), 515–519.

Ciani, C., Pistorio, G., Mearelli, M., & Falcone, C. (2023). Immunofluorescence protocol for localizing protein targets in brain tissue from diverse model and non-model mammals. *STAR Protocol*, **4**(3), 102482.

Clarac, F., Brocard, F., & Vinay, L. (2004). The maturation of locomotor networks. In *Progress in brain research* (Vol. **143**, pp. 57–66). Elsevier.

Cotrina, M. L., Lin, J. H., López-García, J. C., Naus, C. C., & Nedergaard, M. (2000). ATP-mediated glia signaling. *Journal of Neuroscience*, **20**(8), 2835–2844.

Danneman, P. J., & Mandrell, T. D. (1997). Evaluation of five agents/methods for anesthesia of neonatal rats. *Laboratory Animal Science*, **47**(4), 386–395.

Delpire, E., & Staley, K. J. (2014). Novel determinants of the neuronal Cl^- concentration. *The Journal of Physiology*, **592**(19), 4099–4114.

Deumens, R., Mazzone, G. L., & Taccola, G. (2013). Early spread of hyperexcitability to caudal dorsal horn networks after a chemically-induced lesion of the rat spinal cord in vitro. *Neuroscience*, **229**, 155–163.

Ditunno, J. F., Little, J. W., Tessler, A., & Burns, A. S. (2004). Spinal shock revisited: A four-phase model. *Spinal Cord*, **42**(7), 383–395.

Etlin, A., Blivis, D., Ben-Zwi, M., & Lev-Tov, A. (2010). Long and short multifunicular projections of sacral neurons are activated by sensory input to produce locomotor activity in the absence of supraspinal control. *Journal of Neuroscience*, **30**(31), 10324–10336.

Fields, R. D., & Stevens, B. (2000). ATP: An extracellular signaling molecule between neurons and glia. *Trends in Neuroscience (Tins)*, **23**(12), 625–633.

Garcia-Elias, A., Mrkonjić, S., Jung, C., Pardo-Pastor, C., Vicente, R., & Valverde, M. A. (2014). The TRPV4 channel. In B. Nilius & V. Flockerzi (Eds.), *Mammalian transient receptor potential (TRP) cation channels* (pp. 293–319). Springer Berlin Heidelberg.

Goldberg, M. E. (2015). Response to protocol review scenario: Protocol is acceptable. *Laboratory Animals*, **44**(6), 204–205.

Goncharenko, K., Eftekharpour, E., Velumian, A. A., Carlen, P. L., & Fehlings, M. G. (2014). Changes in gap junction expression and function following ischemic injury of spinal cord white matter. *Journal of Neurophysiology*, **112**(9), 2067–2075.

Grillner, S., McClellan, A., & Sigvardt, K. (1982). Mechanosensitive neurons in the spinal cord of the lamprey. *Brain Research*, **235**(1), 169–173.

Guedes, R. C., & do Carmo, R. J. (1980). Influence of ionic disturbances produced by gastric washing on cortical spreading depression. *Experimental Brain Research*, **39**(3), 341–349.

Hong, Z., Tian, Y., Qi, M., Li, Y., Du, Y., Chen, L., Liu, W., & Chen, L. (2016). Transient receptor potential vanilloid 4 inhibits γ-aminobutyric acid-activated current in hippocampal pyramidal neurons. *Frontiers in Molecular Neuroscience*, **9**, 77.

Jenkins, B. A., & Lumpkin, E. A. (2017). Developing a sense of touch. *Development (Cambridge, England)*, **144**(22), 4078–4090.

Kanju, P., & Liedtke, W. (2016). Pleiotropic function of TRPV4 ion channels in the central nervous system. *Experimental Physiology*, **101**(12), 1472–1476.

Kumar, H., & Han, I. (2022). The neuroscience of transient receptor potential vanilloid type 4 (TRPV4) and spinal cord injury. In *Cellular, molecular, physiological, and behavioral aspects of spinal cord injury* (pp. 229–238). Elsevier.

Kumar, H., Lim, C. S., Choi, H., Joshi, H. P., Kim, K.-T., Kim, Y. H., Park, C. K., Kim, H. M., & Han, I. B. (2020). Elevated TRPV4 levels contribute to endothelial damage and scarring in experimental spinal cord injury. *Journal of Neuroscience*, **40**(9), 1943–1955.

Lakke, E. A. (1997). The projections to the spinal cord of the rat during development: A timetable of descent. *Advances in Anatomy, Embryology and Cell Biology*, **135**, I-XIV, 1–143.

Leao, A. A. (1944). Spreading depression of activity in the cerebral cortex. *Journal of Neurophysiology*, **7**(6), 359–390.

Liu, D., Thangnipon, W., & McAdoo, D. J. (1991). Excitatory amino acids rise to toxic levels upon impact injury to the rat spinal cord. *Brain Research*, **547**(2), 344–348.

Marques-Smith, A., Lyngholm, D., Kaufmann, A. K., Stacey, J. A., Hoerder-Suabedissen, A., Becker, E. B., Wilson, M. C., Molnár, Z., & Butt, S. J. (2016). A transient translaminar GABAergic interneuron circuit connects thalamocortical recipient layers in neonatal somatosensory cortex. *Neuron*, **89**(3), 536–549.

Mayer, M. L., & Westbrook, G. L. (1987). The physiology of excitatory amino acids in the vertebrate central nervous system. *Progress in Neurobiology*, **28**(3), 197–276.

Mazzone, G. L., Mohammadshirazi, A., Aquino, J. B., Nistri, A., & Taccola, G. (2021). GABAergic mechanisms can redress the tilted balance between excitation and inhibition in damaged spinal networks. *Molecular Neurobiology*, **58**(8), 3769–3786.

McAdoo, D. J., Robak, G., Xu, G.-Y., & Hughes, M. G. (2000). Adenosine release upon spinal cord injury. *Brain Research*, **854**(1–2), 152–157.

McAdoo, D. J., Xu, G.-Y., Robak, G., & Hughes, M. G. (1999). Changes in amino acid concentrations over time and space around an impact injury and their diffusion through the rat spinal cord. *Experimental Neurology*, **159**(2), 538–544.

Mertens, M., Kessels, S., Veeningen, N., Scheijen, E. E. M., Mussen, F., Delbroek, A., Van Broeckhoven, J., Alpizar, Y. A., & Brône, B. (2025). Loss of TRPV4 is insufficient to promote repair in a spinal cord injury contusion model. *Scientific Reports*, **15**(1), 26757.

Michinaga, S. (2024). Drug discovery research for traumatic brain injury focused on functional molecules in astrocytes. *Biological & Pharmaceutical Bulletin*, **47**(2), 350–360.

Mohammadshirazi, A., Apicella, R., Zylberberg, B. A., Mazzone, G. L., & Taccola, G. (2023). Suprapontine structures modulate brainstem and spinal networks. *Cellular and Molecular Neurobiology*, **43**(6), 2831–2856.

Mohammadshirazi, A., Mazzone, G. L., Zylberberg, B. A., & Taccola, G. (2025). A focal traumatic injury to the neonatal rodent spinal cord causes an immediate and massive spreading depolarization sustained by chloride ions, with transient network dysfunction. *Cellular and Molecular Neurobiology*, **45**(1), 10.

Musienko, P., van den Brand, R., Marzendorfer, O., Roy, R. R., Gerasimenko, Y., Edgerton, V. R., & Courtine, G. (2011). Controlling specific locomotor behaviors through multidimensional monoaminergic modulation of spinal circuitries. *Journal of Neuroscience*, **31**(25), 9264–9278.

Phifer, C. B., & Terry, L. M. (1986). Use of hypothermia for general anesthesia in preweanling rodents. *Physiology & Behavior*, **38**(6), 887–890.

Qi, M., Wu, C., Wang, Z., Zhou, L., Men, C., Du, Y., Huang, S., Chen, L., & Chen, L. (2018). Transient receptor potential vanilloid 4 activation-induced increase in glycine-activated current in mouse hippocampal pyramidal neurons. *Cellular Physiology and Biochemistry*, **45**(3), 1084–1096.

Shatillo, A., Salo, R. A., Giniatullin, R., & Gröhn, O. H. (2015). Involvement of NMDA receptor subtypes in cortical spreading depression in rats assessed by fMRI. *Neuropharmacology*, **93**, 164–170.

Somjen, G. G. (2015). Mechanisms of spreading depression and hypoxic spreading depression-like depolarization. *Physiological Reviews*, **81**(3), 1065–1096.

Stein, W., DeMaegd, M. L., Braun, L. Y., Vidal-Gadea, A. G., Harris, A. L., & Städele, C. (2022). The dynamic range of voltage-dependent gap junction signaling is maintained by Ih-induced membrane potential depolarization. *Journal of Neurophysiology*, **127**(3), 776–790.

Stewart, A. N., Jones, L. A. T., & Gensel, J. C. (2022). Improving translatability of spinal cord injury research by including age as a demographic variable. *Frontiers in Cellular Neuroscience*, **16**, 1017153

Sutherland, T. C., Mathews, K. J., Mao, Y., Nguyen, T., & Gorrie, C. A. (2017). Differences in the cellular response to acute spinal cord injury between developing and mature rats highlights the potential significance of the inflammatory response. *Frontiers in Cellular Neuroscience*, **10**, 310.

Taber, K. H., & Hurley, R. A. (2014). Volume transmission in the brain: Beyond the synapse. *JNP*, **26**(1), 1–4.

Taccola, G., Salazar, B. H., Apicella, R., Hogan, M. K., Horner, P. J., & Sayenko, D. (2020). Selective antagonism of A1 adenosinergic receptors strengthens the neuromodulation of the sensorimotor network during epidural spinal stimulation. *Frontiers in Systems Neuroscience*, **14**, 44.

Valle, M. E. D., Cobo, T., Cobo, J. L., & Vega, J. A. (2012). Mechanosensory neurons, cutaneous mechanoreceptors, and putative mechanoproteins. *Microscopy Research and Technique*, **75**(8), 1033–1043.

Vialle, R., Piétin-Vialle, C., Vinchon, M., Dauger, S., Ilharreborde, B., & Glorion, C. (2008). Birth-related spinal cord injuries: A multicentric review of nine cases. *Childs Nervous System*, **24**(1), 79–85.

Wang, M. Y., Hoh, D. J., Leary, S. P., Griffith, P., & McComb, J. G. (2004). High rates of neurological improvement following severe traumatic pediatric spinal cord injury. *Spine*, **29**(13), 1493–1497.

Wei, X., Edelmayer, R. M., Yan, J., & Dussor, G. (2011). Activation of TRPV4 on dural afferents produces headache-related behavior in a preclinical rat model. *Cephalalgia*, **31**(16), 1595–1600.

Xu, G. (2004). Concentrations of glutamate released following spinal cord injury kill oligodendrocytes in the spinal cord. *Experimental Neurology*, **187**(2), 329–336.

Zhang, X., Levy, D., Noseda, R., Kainz, V., Jakubowski, M., & Burstein, R. (2010). Activation of meningeal nociceptors by cortical spreading depression: Implications for migraine with aura. *Journal of Neuroscience*, **30**(26), 8807–8814.

Additional information

Data availability statement

Datasets generated and/or analysed in the current study are available from the corresponding author upon reasonable request.

Competing interests

The authors declare that they have no competing interests. The impactor adopted in the study is currently being patented by SISSA and is available upon request.

Author contributions

G.T. contributed to the study conception and design. A.M., C.C. and F.E.M. performed experiments. A.M., C.C., F.E.M. and G.T. were responsible for material preparation, data collection and analysis. G.T. was responsible for the first draft of the manuscript. A.M. was was responsible for the illustrations. A.M., C.F. and R.G. commented on previous versions of the manuscript. All authors approved the final version of the manuscript submitted for publication.

Acknowledgements

GT is grateful to Mrs Elisa Ius for her excellent assistance in preparing the manuscript and to John Fischetti for technical support in fabricating the impactor. The study was supported by intramural SISSA grants through the 5xMILLE2020 framework. CF, CC and FEM are grateful for Human Technopole Early Career Fellowship grant support awarded to CF.

Open access publishing facilitated by Scuola Internazionale Superiore di Studi Avanzati, as part of the Wiley - CRUI-CARE agreement.

Keywords

isolated CNS, mechanoreceptors, motor evoked potentials, neonatal SCI, spinal shock

Supporting information

Additional supporting information can be found online in the Supporting Information section at the end of the HTML view of the article. Supporting information files available:

Peer Review History